



HAL
open science

Numerical simulation of liquid metal infiltration and solidification inside a capillary tube

Nadine Moussa, Hervé Duval, Dominique Gobin, Benoît Goyeau

► **To cite this version:**

Nadine Moussa, Hervé Duval, Dominique Gobin, Benoît Goyeau. Numerical simulation of liquid metal infiltration and solidification inside a capillary tube. HEFAT2014 10th International Conference on Heat Transfer, Fluid Mechanics and Thermodynamics, Jul 2014, Orlando, United States. hal-01809827

HAL Id: hal-01809827

<https://hal.science/hal-01809827>

Submitted on 7 Jun 2018

HAL is a multi-disciplinary open access archive for the deposit and dissemination of scientific research documents, whether they are published or not. The documents may come from teaching and research institutions in France or abroad, or from public or private research centers.

L'archive ouverte pluridisciplinaire **HAL**, est destinée au dépôt et à la diffusion de documents scientifiques de niveau recherche, publiés ou non, émanant des établissements d'enseignement et de recherche français ou étrangers, des laboratoires publics ou privés.

NUMERICAL SIMULATION OF LIQUID METAL INFILTRATION AND SOLIDIFICATION INSIDE A CAPILLARY TUBE

Moussa N.^{1, 2*}, Duval H.¹, Gobin D.² and Goyeau B.²

¹LGPM Ecole Centrale Paris,
Grande Voie des Vignes,
92295 Châtenay-Malabry Cedex,
France,

²EM2C Ecole Centrale Paris,
Grande Voie des Vignes,
92295 Châtenay-Malabry Cedex,
France,

*Author for correspondence
E-mail: nadine.moussa@ecp.fr

ABSTRACT

A metal foam is a porous structure whose solid matrix has a large fraction of interconnected cells. The objective of our study is to define a new manufacturing process via casting that produces homogenous open cell metal foams. This comes down to studying the infiltration and solidification process of a liquid metal inside a porous mould. The metal foams are characterized by their high porosity and permeability values; thus, the size of the mould pore is small enough to be considered as a capillary tube. Therefore, the focus of this paper is on modelling and numerical simulation at a local scale of the infiltration and solidification of liquid metal inside a capillary tube.

The main difficulty lies in the presence of 4 phases; mould, air, liquid and solid metal: a one-domain approach is chosen in the modelling of the problem. We subsequently obtained one set of equations as a function of two volumetric fractions: the metal/air fraction in the pore and the liquid fraction in the metal. Before the solidification starts, the liquid metal infiltrates the capillary thus the liquid metal-gas interface must be tracked. This is done implicitly using the VOF (Volume Of Fluid) method [1], where the advection equation of the volumetric metal fraction is coupled to the Navier-Stokes equation. The solidification process of the liquid metal is accounted for using the enthalpy-porosity approach [2- 3]. In addition, to ensure a zero velocity field in the mould and in the

solid metal, two penalty coefficients as a function of the phase indicators were added to the momentum equation.

The above mathematical model is implemented in a CFD tool: OpenFOAM [4]. A numerical validation is performed by comparing the numerical results with well-known solutions of test cases. Then, the numerical results of the liquid aluminium solidification are compared to the fluidity tests carried out experimentally. Subsequently, a numerical parametrical study enabled us to find the relationships between the distance flowed by the liquid before its solidification and the infiltration time as function of the pressure difference, heat transfer coefficient and metal superheat.

In our future work, we will derive a macroscopic model at the mould scale by up-scaling: the volume-averaged equations will be obtained from the local scale model using the volume averaging method [5]. Then, the numerical results will be compared to the metal foam casting tests.

INTRODUCTION

The competitiveness in the metal industry result of severe products specifications in order to reduce the cost of the manufacturing processes. Thus, metal foam presents a promising material that keeps the high mechanical properties of the metal while reducing the weight up to 90%. Metal foam has

variety of applications depending on whether the cells are connected or not; e.g. open-cells foam are used in heat exchanger to increase heat transfer, while closed-cells foam are employed as impact-absorbing material such in vehicle's crash box. Several patented manufacturing processes have been introduced during the last two decades. We count: Alporas® by Shinko Wire Co. Ltd.[6], Alusion™ by CYMAT [7], Duocel® foam by ERG aerospace cooperation [8]. However, the metallic melts are foamed or by injecting gas into liquid or by the use of blowing agents and normally these processes need a stabilizing mechanism. As a result, the products are not homogenous, thus the geometry and physical properties cannot be controlled. Therefore, the CTIF[9] presented a manufacturing process of metal foam via casting, i.e. CastFoam®[10] that produce a well defined homogenous foams. However, this process needs to be elaborated before being employed in the metal industry. Thus, the infiltration and solidification of liquid metal inside the porous mould should be studied. Metal foams obtained using this process, have high permeability and porosity values; hence the size of the mould pore is small and can be modelled as a capillary tube. Subsequently, our objective is to study the infiltration and solidification of liquid metal in a capillary tube.

NOMENCLATURE

ρ	[kg/m ³]	Density
μ	[Pa.s]	Dynamic viscosity
k	[W/mK]	Thermal conductivity
cp	[J/kgK]	Heat capacity
σ	[N/m]	Surface tension
K	[m ⁻¹]	Curvature
\mathbf{v}	[m/s]	Velocity vector
p	[Pa]	Pressure
T	[K]	Temperature
H	[KJ/ m ³]	Enthalpy
L	[J/ m ³ K]	Latent heat
L_m	[m]	Mechanical entrance length
L_{th}	[m]	Thermal entrance length
D	[m]	Tube diameter
r	[m]	Radius
Re	[-]	Reynolds number
Pe	[-]	Peclet number
Nu	[-]	Nusselt number
Special characters		
α	[-]	Metal volume fraction
g^l	[-]	Liquid metal volume fraction
ε	[-]	Fluid indicator phase
A	[kg/m ³ s]	Solid metal penalty coefficient
B	[kg/m ³ s]	Mould penalty coefficient
C	[kg/m ³ s]	Large constant (~10 ⁶)
D	[kg/m ³ s]	Large constant (~10 ⁹)
b	[-]	Small numerical constant (10 ⁻³)
Subscripts		
l		Liquid metal
s		Solid metal
$metal$		Metal
g		Gas
m		Mould
r		Relative
ref		Reference
in		Inlet
out		Outlet

MATHEMATICAL MODEL

The liquid metal infiltration and solidification inside a capillary tube is handled by solving the governing equations presented in this section, using a one-domain approach. The fluid flow is governed by the Navier-Stokes equations for an incompressible fluid. Therefore, the continuity and the momentum equations are given by:

$$\frac{\partial \rho}{\partial t} + \nabla \cdot (\rho \mathbf{v}) = 0 \quad (1)$$

$$\frac{\partial \rho \mathbf{v}}{\partial t} + \nabla \cdot (\rho \mathbf{v} \mathbf{v}) = -\nabla p + \nabla (\mu \nabla \mathbf{v}) + \sigma K \nabla \alpha - A \mathbf{v} - B \mathbf{v} \quad (2)$$

$$\text{With } K = -\nabla \cdot \left(\frac{\nabla \alpha}{|\nabla \alpha|} \right), \text{ curvature of the metal-gas interface}$$

In two-phase flow model the momentum equation contains an additional source term which is the pressure jump at the liquid-gas interface arisen from the surface tension between the two fluids. Using the volume-of-fluid (VOF) method[1] this term that is the third term in the r.h.s. of equation (2) is evaluated by resolving the transport equation of the metal volumetric fraction α :

$$\frac{\partial \alpha}{\partial t} + \nabla \cdot (\mathbf{v} \alpha) + \nabla \cdot [\mathbf{v}_r \alpha (1 - \alpha)] = 0 \quad (3)$$

$$\text{With } \mathbf{v}_r = \mathbf{v}_l - \mathbf{v}_g, \text{ the relative velocity}$$

The surface curvature is function of volumetric fraction and is required for the determination of surface tension force. Therefore, the calculation of the volumetric fraction distribution must be accurate especially in case of high physical properties ratios i.e. density, thermal conductivity..., where small errors in evaluating the volumetric fraction leads to significant errors in calculating the effective physical properties. Thus, equation (3) contains an additional convective term known as the compression term active only within the interface region $\alpha(1-\alpha)$; its role is to get a sharper liquid-gas interface. As we can see, the momentum equation contains also two supplementary artificial terms, which will be discussed later on after presenting the solidification model.

The modelling of convection-diffusion phase change of the metal is done using a modified enthalpy-porosity method[2]. The advantage of this method is that it respects the one domain approach. The method is modified by writing the energy equation as function of temperature instead of enthalpy and is extended by a continuous liquid fraction function, i.e. error function[3]. The energy conservation equation is written as follow:

$$\frac{\partial H}{\partial t} + \nabla \cdot (\mathbf{v} H) = \nabla \cdot (k \nabla T) \quad (4)$$

The latter contains two unknowns, fortunately the enthalpy can be written as function of the temperature and the volumetric fractions: α the metal/air fraction, g_l the liquid fraction in the metal and ε the fluid phase indicator.

$$H = \varepsilon \left[\alpha \left(g_l \int_{T_{ref}}^T \rho_l c_{p_l} d\theta + \rho_l g_l L + (1 - g_l) \int_{T_{ref}}^T \rho_s c_{p_s} \right) + (1 - \alpha) \int_{T_{ref}}^T \rho_g c_{p_g} d\theta \right] + (1 - \varepsilon) \left[\int_{T_{ref}}^T \rho_m c_{p_m} d\theta \right] \quad (5)$$

Replacing the enthalpy with its expressions in equation (4), and neglecting the density change between the liquid and solid phases of the metal, we get the following energy equation:

$$\rho c_p \frac{\partial T}{\partial t} + \rho c_p \nabla \cdot (\mathbf{v}T) = \nabla \cdot (k \nabla T) - \alpha \rho_{metal} \left(\int_{T_{ref}}^T (c_{p_l} - c_{p_s}) d\theta + L \right) \left(\frac{\partial g_l}{\partial t} + \mathbf{v} \nabla g_l \right) \quad (6)$$

As we mentioned earlier, the liquid fraction is considered to be a continuous function of temperature given by:

$$g_l = \frac{1}{2} \operatorname{erf} \left(\frac{8(T - T_{melt})}{T_{fusion}} \right) + \frac{1}{2} \quad (7)$$

With T_{melt} and T_{fusion} being reciprocally the arithmetic mean and the difference between liquidus and solidus temperatures of the metal in question. After replacing the liquid volumetric fraction g_l with its expression in equation (6), the energy conservation equation is function of one unknown, the temperature.

In a one domain approach, the four phases; mould, air, liquid and solid metal are considered as one effective fluid throughout the domain having physical properties weighted as function of the phase fractions.

$$\rho = \alpha \rho_{metal} + (1 - \alpha) \rho_g \quad (8)$$

$$\mu = \alpha \mu_l + (1 - \alpha) \mu_g \quad (9)$$

$$\rho c_p = \varepsilon \left[\alpha \rho_{metal} (g_l c_{p_l} + (1 - g_l) c_{p_s}) + (1 - \alpha) \rho_g c_{p_g} \right] + (1 - \varepsilon) \left[\rho_m c_{p_m} \right] \quad (10)$$

These effective properties are obtained by supposing a linear variation between the physical properties of each phase at the different interfaces. However, this simple relation cannot be used when calculating the effective conductivity because of the

high ratio between the metal and air conductivity values. Therefore, using Patankar[11] formulation, the effective conductivity is given by:

$$k = \varepsilon \left[\frac{\alpha}{(g_l k_l + (1 - g_l) k_s)} + \frac{(1 - \alpha)}{k_g} \right]^{-1} + (1 - \varepsilon) [k_m] \quad (11)$$

Now, reviewing the momentum equation, two sources terms were added, they were derived from the Carman-Kozeny equations for flow in a porous media. Therefore, the condition of zero velocity fields in the solidified metal is verified using the penalty coefficient A that acts only in the metal region and is function of the liquid metal volumetric fraction:

$$A = \alpha \varepsilon C \frac{(1 - g_l)^2}{g_l^3 + b} \quad (12)$$

When the calculated temperature T is higher than the melting temperature, the liquid fraction is equal to 1 and the penalty coefficient vanishes, thus the momentum equation returns to its normal form. However, when the calculated temperature is lower than the melting temperature, solidification process occurs, and the liquid fraction is equal to zero. Thus, the penalty coefficient has a large value that multiplies the velocity vector which result in a zero velocity field. The constant b has a small value; its role is to avoid division by zero.

The second additional source term in the momentum equation, is to ensure a zero velocity field in the mould region. Thus, the penalty coefficient is function of the fluid phase indicator:

$$B = (1 - \varepsilon) D \quad (13)$$

In the fluid region ε equal 1 and the penalty coefficient turns to zero. However, in the mould region ε equal 0 and the penalty coefficient has a large value multiplying the velocity vector therefore insuring a zero velocity solution.

NUMERICAL VALIDATION

The mathematical model presented earlier was implemented in a CFD open source software OpenFOAM [4]. The latter is written in C++ for linux operating systems, and contains essential codes to solve flow and heat transfer problems. It uses the finite volume method where the space is divided into discrete control volumes, and time is split into a number of time-steps. The solution procedure of the transition simulations can be summarized as follow: first the mesh is generated, and the variable fields are initialized. After that, the time loop starts, and the time step is calculated in order to verify the Courant-Friedrichs-Lewy (CFL) condition. Then, the transport equation

of the metal volumetric fraction (3) is solved which enables us to calculate the surface tension force. Subsequently, the metal-gas interface is constructed and the physical properties are updated as function of volumetric fractions (equations (8, 9, 10 & 11)). Next, the pressure-velocity coupling is done using the PIMPLE (PISO-SIMPLE) scheme of OpenFOAM where the continuity and the momentum equations (1, 2) are solved. Afterwards, the convergence of the solution is monitored by calculating the continuity error. At this stage, the pressure and velocity fields as well as the metal volumetric fraction distribution are known for the current time step. Using the velocity field solution, the energy equation (6) can now be solved in order to obtain the temperature field and the metal liquid volumetric fraction g_l , which will be used to update the penalty source term of the momentum equation. Now all the variable fields are known, if the final time is not reached yet, the time loop continues with the calculation of the next time step.

The numerical validation of the code is done by comparing the numerical solutions with analytical solutions and correlations of test cases available in the literary. In this section, the mould is not taken into consideration. Therefore, the capillary tube is modelled as a cylindrical tube of 1.2 mm radius, and 120 mm length. The mesh is structured 2D radial quadrangle extruded to 3D using Salome software[12], and is shown in the figure below.

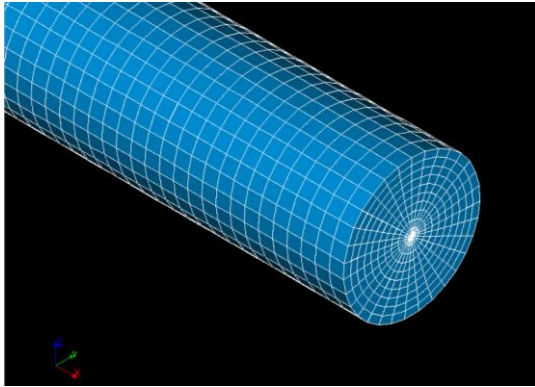


Figure 1 Global view of the geometry and mesh of the tube

One phase flow

The first step of our code validation is by simulating an isothermal one phase flow and comparing it to the Poiseuille solution. This is done by fixing the right thermal conditions. Thus, the tube is initially filled with liquid aluminium at a temperature higher than its fusion temperature and a zero thermal flux is set at the tube wall. A Dirichlet boundary condition of constant uniform velocity profile is imposed at the inlet and an absolute pressure value of 0 Pa is fixed at the outlet. The adimensional number of Reynolds is taken to have a value of 600, which corresponds to an average velocity of 0.1 m/s. The entrance length after which the flow is fully developed is calculated as follow:

$$L_m = 0.0576 \text{Re} D \quad (14)$$

The radial velocity profile at an axial section farther from the entrance length ($x=100\text{mm}$) is compared to the Poiseuille solution and shown in Figure 2. Both solutions are in good agreement, and the relative error at the tube axe is less than 1%.

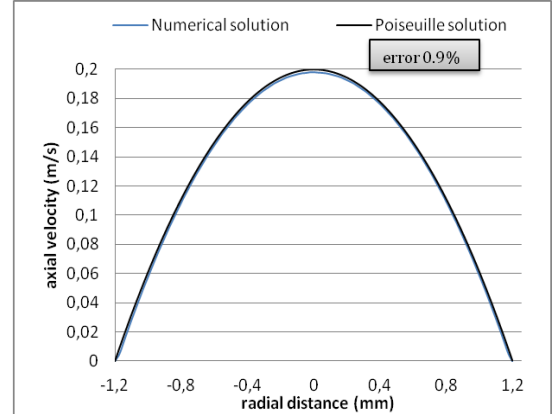


Figure 2 axial velocity profile at $x=100\text{mm}$

For an internal forced convection, there are two possibilities of thermal conditions at the tube wall: fixed temperature or constant thermal flux, accordingly to which the thermal entrance length and the correlated dimensionless number of Nusselt are given. Using the aluminium properties, the thermal entrance length for both cases is negligible in comparison with the mechanical one. In addition, the high thermal conductivity of the aluminium yields to a uniform radial thermal profile in the case of fixing a constant temperature at the wall. Therefore, the validation of the thermal behaviour is done by fixing a constant flux at the wall. In order, to identify the value of the flux that must be used as a boundary condition; the energy that should be extracted from the metal in order to lower its temperature from T_{in} to T_{out} is calculated.

For a constant heat flux at the wall, we have [13]:

$$\frac{L_{th}}{DPe} = \begin{cases} 0.053Pe = 0.7 \\ 0.043Pe = \infty \end{cases} \quad (15)$$

And

$$Nu = \frac{48}{11} = 4.363 \quad (16)$$

The temperature radial profile obtained at ($x=100\text{mm}$) is shown in Figure 3 and gives the following Nusselt number:

$$Nu = 4.3 \quad (17)$$

Comparing it with the correlated Nusselt number yields to a relative error of 1.45%.

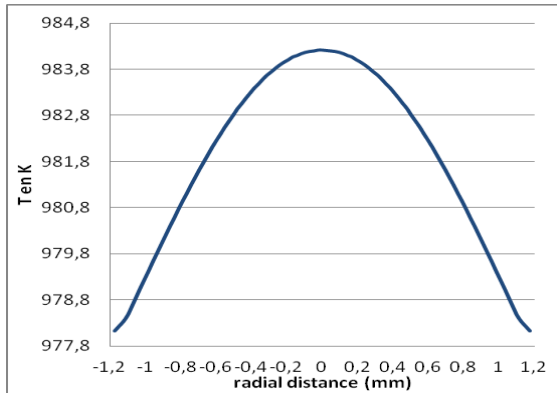


Figure 3 Temperature radial profile at $x=100\text{mm}$

In the previous thermal simulation the heat flux imposed at the tube wall, was sufficient enough to lower the liquid aluminium temperature in order to calculate the Nusselt number once the mechanical and thermal regime are established but not high enough to induct the solidification of the metal liquid. Now, in order to observe the solidification phenomena of the liquid flowing inside the tube, the heat flux imposed at the tube wall is much higher. The tube is initially filled with liquid aluminium at a temperature of 1073 K, driven by a pressure difference of 300 Pa between the inlet and outlet. The evolution of the liquid fraction is shown in the pictures below:



Figure 4 solidification process of liquid aluminium (in red liquid phase, in blue solid phase); a- at start time the tube is completely filled by liquid aluminium, b- the aluminium solidification starts at the tube wall at a distance from the entry, c- the solidified aluminium progress in the radial direction, d- the solidified aluminium close the tube at a section further from the entrance and stops the fluid flow, e- the solidification progress at the entry direction, f- at the end the aluminium is completely solidified

The solidification process of the liquid aluminium cannot be validated by an analytical solution, but the numerical results show a correct physical behaviour.

Two phase flow

At this stage, the solidification code should be tested in simulating the infiltration and solidification process of liquid metal into the capillary tube. For an isothermal two-phase flow, special attention is given to the interface velocity. In fact, after a certain time the interface shape remains the same. This means, that the interface can be considered as a solid part where all the particles move at the same velocity, which

corresponds necessarily to the fluid mean velocity; as Dussan states in her article [14] “the speed of the contact line $\frac{Q}{\pi a^2}$ ”. In order to understand the motion of the two fluids and the interface dynamic we refer to the article mentioned earlier [14]; where it is demonstrated that the displacing fluid undergoes a rolling motion and that the displaced fluid has a similar but more complex behaviour. To visualize this, the relative velocity vectors in the interface frame of reference are shown below:

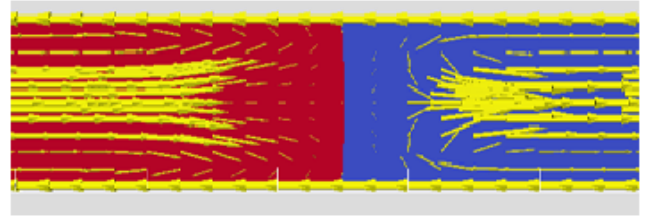


Figure 5 Relative velocity vectors in the region of the liquid-gas interface

Figure 5 shows that the displacing fluid flows forward at the tube centre, and then rolls at the interface vicinity to flows backward near the wall. At the other hand, the displaced fluid flows backward near the wall, and rolls at the interface to flows forward at the tube centre.

For an internal convection two-phase flow, the tube wall is considered as adiabatic, and the two fluids have different temperatures that are higher than the solidification temperature of the aluminium. The liquid aluminium infiltrating the tube cools down by losing its energy to the air that has a lower temperature.

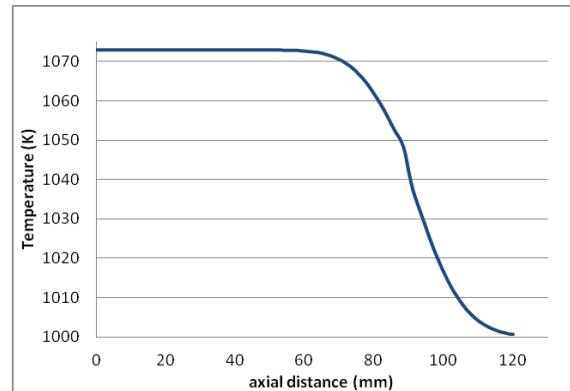


Figure 6 Axial temperature profile

As mentioned earlier, the solidification cases cannot be validated by analytical comparison. However, it is of our interest to observe the solidification process of the liquid aluminium infiltrating the tube. That is why, in this section we are going to show the solidification behaviour of the liquid aluminium under an imposed negative flux boundary condition. In aim to eliminate the air temperature effect on the solidification kinetics of the liquid aluminium, the latter is taking to be equal to the liquid aluminium temperature $T=1073\text{K}$.

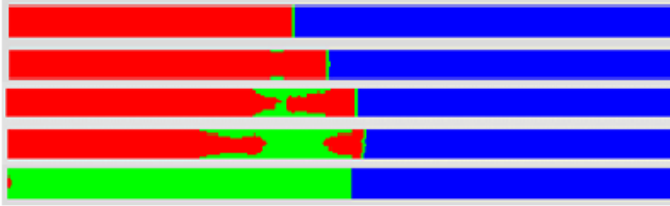


Figure 7 liquid aluminium solidification progress; a- the liquid aluminium infiltrates the tube, b- the solidification starts at the wall behind the interface, c- the solidified aluminium closes the flow passage, d- the solidification propagates in both directions, the interface oscillates, e- at the end the aluminium is completely solidified

RESULTS AND DISCUSSIONS

REFERENCES

- [1] H. Rusche, Computational Fluid Dynamics of Dispersed Two-Phase Flows at High Phase Fractions, 2002
- [2] A. D. Brent, V. R. Voller, and K. J. Reid, The Enthalpy-Porosity Technique For Modeling Convection-Diffusion Phase Change: Application To The Melting Of A Pure Metal, *Numer. Heat Transf.*, vol. 13, 1988, pp. 297–318
- [3] F. Rösler and D. Brüggemann, Shell-and-tube type latent heat thermal energy storage: numerical analysis and comparison with experiments, *Heat Mass Transf.*, vol. 47, no. 8, Jul. 2011, pp. 1027–1033
- [4] www.openfoam.com
- [5] Whitaker Stephen, The Method of Volume Averaging, *Kluwer Academic Publishers*, 1999
- [6] T. Miyoshi, M. Itoh, S. Akiyama, and A. Kitahara, ALPORAS Aluminum Foam: Production Process, Properties, and Applications, *Adv. Eng. Mater.*, vol. 2, no. 4, 2000, pp. 179–183
- [7] www.alusion.com/home.html
- [8] www.ergaerospace.com/index.html
- [9] www.ctif.com
- [10] www.alveotec.fr/innovation.html
- [11] Suhas V. Patankar, Numerical Heat Transfer and Fluid Flow. *Taylor & Francis Group LLC*, 1980
- [12] www.salome-platform.org
- [13] J. Padet, Convection thermique et massique Nombre de Nusselt: partie 1, *Tech. l'ingénieur*, vol. 33
- [14] E. B. Dussan V., On the spreading of liquids on solid surfaces: static and dynamic contact lines, *Annu. Rev. Fluid Mech.*, vol. 11, 1979, pp. 371–400